Positional Control of Crystal Grains in Silicon Thin Film Utilizing Cage-Shaped Protein

2011 Jpn. J. Appl. Phys. 50 04DL12

(http://iopscience.iop.org/1347-4065/50/4S/04DL12)

Japanese Journal of Applied Physics **50** (2011) 04DL12 **REGULAR PAPER**
DOI: 10.1143/JJAP.50.04DL12

Positional Control of Crystal Grains in Silicon Thin Film Utilizing Cage-Shaped Protein

Yosuke Tojo[1]*, Atsushi Miura[1,2], Ichiro Yamashita[1,3,4], and Yukiharu Uraoka[1,4]

[1]*Nara Institute of Science and Technology, Ikoma, Nara 630-0192, Japan*
[2]*National Chiao Tung University, Hsinchu 30010, Taiwan*
[3]*Panasonic, Seika, Kyoto 619-0237, Japan*
[4]*CREST-JST, Kawaguchi, Saitama 331-0012, Japan*

Received September 20, 2010; revised November 15, 2010; accepted November 17, 2010; published online April 20, 2011

We have proposed a new crystallization method for silicon thin films utilizing a cage-shaped protein (ferritin), called "bio-nano crystallization", which combines semiconductor processing technology and biotechnology. We utilized nickel nanoparticle-accommodated ferritins as metal catalysts, and succeeded in performing the crystallization. When the ferritin was adsorbed randomly onto the film, crystal nuclei were formed at random places, thus grain position was randomly distributed. In this study, we performed the positional controlled deposition of ferritin by electrostatic interaction for location control of crystal grains. Positively charged areas were formed on negatively charged SiO_2 using 3-amino-propyltriethoxysilane (APTES) as the electrostatic pattern. As a result, we could optimize Ni ferritin concentration to make a large adsorption difference between APTES and amorphous silicon. Therefore, nickel nanoparticles adsorption areas were controlled using APTES patterns. Furthermore, the location control of crystallized areas was achieved by optimizing the concentration of Ni ferritin and the APTES pattern.

1. Introduction

Recently, polycrystalline silicon (poly-Si) thin film transistors (TFTs) are widely used as driving circuits for various kinds of displays. Further technical innovations on display devices such as realization of higher resolution, higher quality, and downsizing are expected for the realization of system on panel. The device performance depends on the quality of poly-Si thin films; thus, improvement of grain size and quality is important. Therefore, crystallization methods have been studied. Metal-induced lateral crystallization (MILC)[1] is one of the crystallization methods utilizing metal catalysts for poly-Si fabrication, where lateral crystallization of amorphous silicon (a-Si) is advanced after crystalline nucleus formation by annealing of a catalyst. As an improved MILC process, we have proposed and demonstrated the utilization of a cage-shaped supramolecular protein. In nature, ferritin accommodates ferrihydrite ($5Fe_2O_3 \cdot 9H_2O$) nanoparticles in its cavity. In addition, it is well known that different kinds of inorganic nanodots, such as iron oxide, cobalt oxide, and compound semiconductors, can be formed in its cavity by biomineralization.[2–5] Our novel MILC utilizes nickel oxide-accommodated ferritins (Ni-Fers) as metal catalysts for the formation of crystalline nuclei. We named this method as "bio-nano crystallization (BNC)". Ni deposition in the BNC process merely requires a very simple solution process such as just applying a drop of Ni ferritin solution. It does not require complicated and expensive process equipment such as high-vacuum systems. Ni nanoparticle accommodated ferritins are adsorbed on the substrate by the self-assembly capability of ferritin. This process achieves very low-concentration Ni catalyst thin-film fabrication; in this film, the concentration of Ni is very low but sufficient to work as a catalyst for MILC; as a result, we can drastically decrease metal impurity concentration.[6] In addition to these advantages, BNC is highly compatible with conventional patterning process. It will enable the formation of micrometer small patterns by combination of the lift-off method and BNC for position selective crystallization. We previously demonstrated the fabrication of poly-Si thin films possessing a several tens of μm crystal grain size by BNC with normal thermal annealing[6] and pulsed rapid thermal annealing.[7,8] However, Ni-Fers were adsorbed at random places on the a-Si surface; thus, crystal grains were also formed in random positions. In this study, we combine BNC and the selective adsorption of ferritin to realize the positional control of crystal grains. We observed the dependence of Ni adsorption density on Ni-Fer concentration with or without electrostatic interaction. The crystal grain density dependence of Ni-Fer concentration and the number of Ni-Fers for single-crystal grain formation has been revealed. The positions of crystal grains have been controlled utilizing electrostatic interaction patterns.

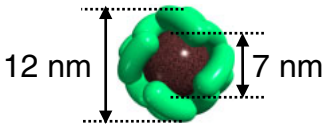

Fig. 1. (Color online) Schematic drawing of ferritin protein.

2. Experimental Methods

Figure 1 depicts a schematic cross-sectional drawing of the ferritin structure. Ferritin has several features, such as its applicability to 1) the formation of different kinds of metal and semiconductor nanodots by replacing Fe;[2,3,9] 2) uniform nanoparticle formation (approximately 7 nm) using the cage-shaped ferritin protein as biotemplates; 3) high-density and selective deposition owing to the ability of self-assembly. Ni accommodated ferritins used as crystalline nuclei of BNC, were synthesized in the vacant cavity of the ferritin protein by biomineralization.[3] The BNC process is schematically depicted in Fig. 2. 50-nm-thick a-Si thin films were deposited by low pressure chemical vapor deposition, and Ni-Fers were adsorbed on a-Si thin films. To form a Ni-Fer monolayer, Ni-Fer solution was drop-cast and incubated on a-Si thin films for adsorption, and spun out in a sealed plastic tube to remove excess proteins. The outer protein shell was removed by oxidation with UV irradiation in ozone atmosphere at 110 °C, and the formation of nickel silicide, which works as a nucleus for lateral crystallization. For the

*E-mail address: t-yosuke@ms.naist.jp

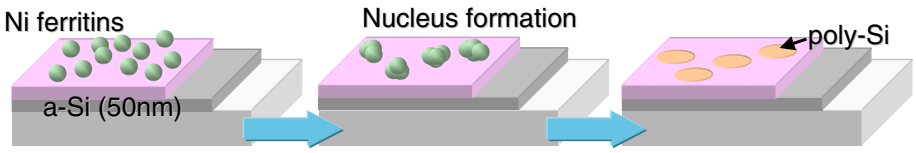

Fig. 2. (Color online) Schematic drawing of bio-nano crystallization process.

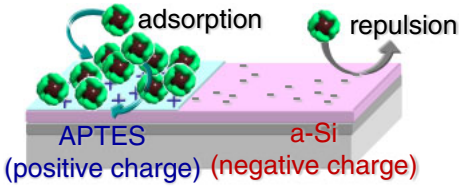

Fig. 3. (Color online) Selective adsorption using 3-amino-propyltriethysilane.

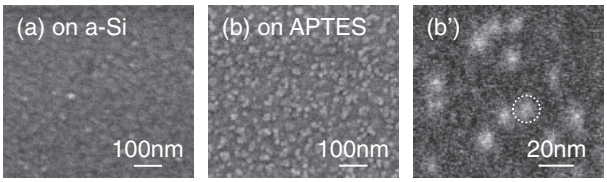

Fig. 4. SEM images of Ni ferritins (0.25 mg/ml, 1 min) on (a) a-Si, (b) APTES, and (b′) magnified image of (b).

crystallization in a-Si, Ni-Fers adsorbed a-Si thin films were annealed at 550 °C for 24 h in N_2 ambient.

The selective adsorption of ferritins was achieved using 3-amino-propyltriethoxysilane (APTES) as the electrostatic adsorption pattern.[10] As shown in Fig. 3, the surfaces of ferritins and SiO_2 have a negative charge; therefore, the electrostatic interaction is repulsive force. On the other hand, APTES has a positive charge. Therefore, it is considered that the selective adsorption of ferritins is realized using APTES islands. APTES as deposited by a vapor process at room temperature for 3 h, and APTES islands were formed by the lift-off process using photolithography (pattern size, 10–100 μm). After the patterning of APTES, ferritins were adsorbed, and the adsorption density of ferritins was observed by scanning electron microscopy (SEM). The crystallinity of crystallized silicon films was estimated by Raman spectroscopy, and crystal grains were observed after secco etching.

3. Results and Discussion

3.1 Adsorption density of Ni-Fers

As mentioned above, it is important that Ni-Fers as metal catalysts were adsorbed at selected areas for crystalline nucleus formation. Therefore, we tried the selective adsorption of Ni-Fers for the realization of the positional control of crystallized areas. It was confirmed that the surfaces of ferritin and SiO_2 are negatively charged, and APTES is positively charged.[11] The APTES layer was formed on the substrate; the selectivity of ferritins was investigated for the positional control of crystal grains. First, Ni-Fer solution (0.25 mg/ml) was dropped on a-Si or APTES, and the adsorption time was from 1 to 10 min. Figure 4 shows images of a sample with adsorbed Ni-Fer with or without APTES, and the Ni ferritin adsorption time was 1 min. Samples were coated with osmium whose thickness was approximately <2 nm for Ni ferritin observation by SEM. The size of single nanoparticles was observed to be approximately 16 nm as shown in Fig. 4(b′). It is consistent with the sum of the thicknesses of the ferritin and osmium-coated thin film. The adsorption densities measured by SEM are summarized in Fig. 5. As shown in Fig. 5(a), the adsorption reactions of ferritin were saturated in 3 min on

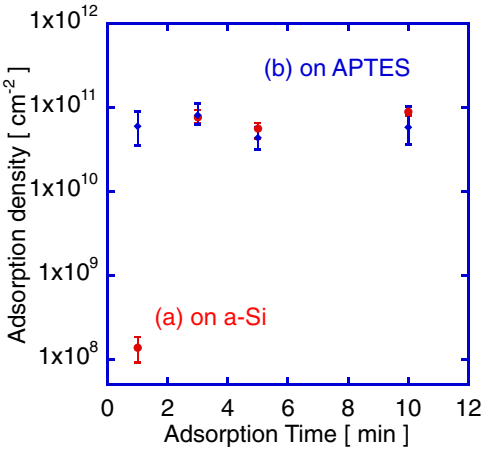

Fig. 5. (Color online) Adsorption density dependence of adsorption time characteristics on (a) a-Si and (b) APTES. (Ni-Fer concentration = 0.25 mg/ml; adsorption times = 1, 3, 5, 10 min).

a-Si, and the adsorption densities were 1.0×10^{11} and 1.0×10^{8} cm^{-2} at 3 and 1 min, respectively. On the other hand, the adsorption density on APTES was 1.0×10^{11} cm^{-2} and saturated in 1 min. It indicates that the adsorption difference can be confirmed by 1 min adsorption time. Therefore we set the adsorption time at 1 min.

Next, the Ni-Fer concentration dependence of the adsorption density is shown in Fig. 6. Ni-Fer concentrations are 0.05, 0.10, 0.25, and 0.50 mg/ml. In the case of a-Si, SEM observation focused on a 16 nm nanoparticle, and Ni-Fers could not be observed by SEM at a low magnification. This suggests that the adsorption densities under 0.10 mg/ml were smaller than approximately 1.0×10^{8} cm^{-2}, as shown in Fig. 6(a). On the other hand, adsorption densities on APTES shown in Fig. 6(b) were higher than those on a-Si. Thus, the selective adsorption of ferritins was achieved utilizing the electrostatic interaction of APTES patterns on the same substrate.

3.2 Ni-Fer concentration dependence on crystal grain positioning, shape, and size

The adsorption densities of Ni-Fers were investigated for crystal grain position control. Therefore, it is necessary to

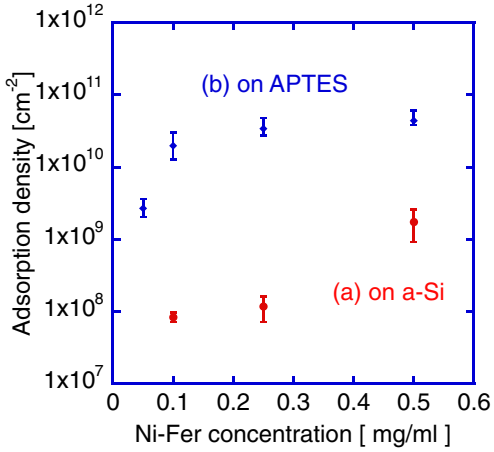

Fig. 6. (Color online) Adsorption density dependence of Ni ferritin concentration characteristics on (a) a-Si and (b) APTES.

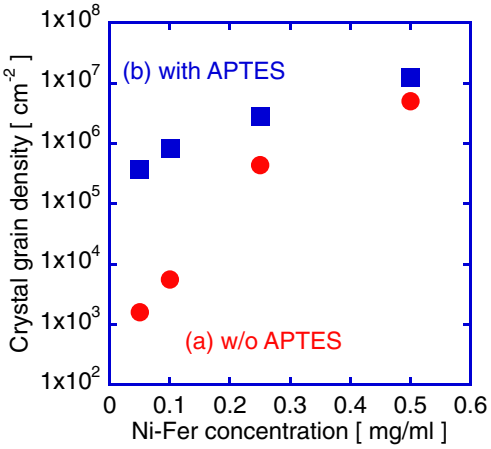

Fig. 8. (Color online) Crystal grain density dependence of Ni ferritin concentration characteristics on (a) a-Si and (b) APTES.

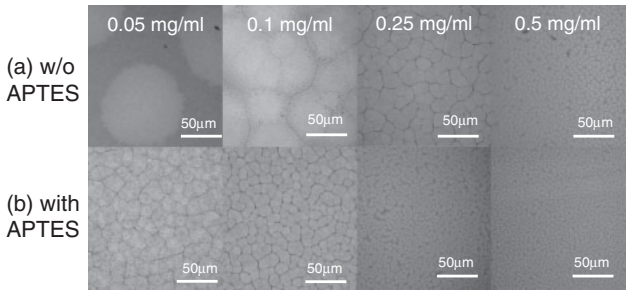

Fig. 7. Crystal grains at 0.05, 0.1, and 0.25 mg/ml (a) without APTES and (b) with APTES.

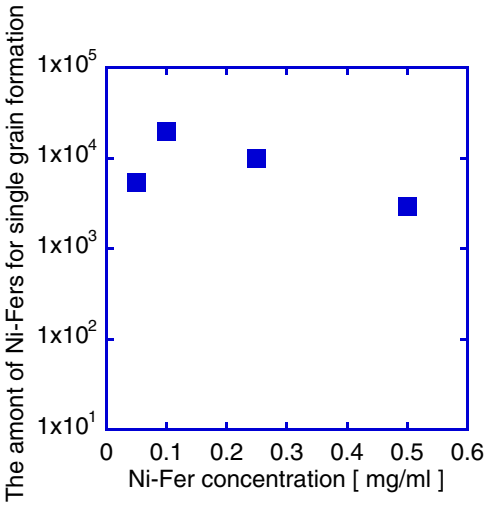

Fig. 9. (Color online) Amount of Ni ferritins for single-grain formation.

investigate the effect of Ni-Fer concentration with APTES on crystal grains shape. We examined the effect of Ni-Fer concentration on crystal grain morphology by depositing Ni-Fers at different concentrations (0.05, 0.10, 0.25, and 0.50 mg/ml) on the film. We simultaneously compared the effect of APTES. Crystallization was carried out at 550 °C for 24 h in N_2 ambient. Crystal grains were observed by optical microscopy after secco etching. Figures 7(a) and 7(b) show without and with APTES treatment on a-Si. The crystal grain sizes are approximately 100 and 20 μm at 0.05 mg/ml without and with APTES, respectively. The observed obvious size difference indicates that the effects of adsorption difference due to APTES on crystal grain size and density. In addition, we observed the decrease in the size and increase in the density of crystal grains with increasing Ni-Fer concentrations.

According to Figs. 6 and 7, it should be noted again that grain size decreased with increasing adsorption density of Ni-Fers, and grain density increased also, as shown in Fig. 8. When the Ni-Fer concentrations were 0.25 and 0.50 mg/ml with APTES treatment, grain densities were little increased from 4.4×10^5 to 2.8×10^6 cm^{-2} and 5.0×10^6 to 1.3×10^7 cm^{-2}, respectively. Therefore, at 0.05 and 0.10 mg/ml, crystal grain densities were increased from 1.6×10^3 to 3.7×10^5 cm^{-2} and 5.6×10^3 to 8.3×10^5 cm^{-2} owing ot the effect of APTES, respectively. As a result, large grain density differences were confirmed in the case of utilizing APTES. To realize positional controlled of crystal grains, a large grains density difference is important. If grain density differences will not change with or without APTES, the effect of APTES on the same substrate can not be confirmed.

The purpose of this study is the positional control of crystallized areas utilizing APTES patterns by controlled Ni-Fer adsorption. Therefore, the importance of the amount of Ni-Fers on APTES was suggested for single-grain formation from Ni-Fer adsorption densities ($D_{\text{Ni-Fers}}$) [Fig. 6(b)] and crystal grain densities (D_{grains}) [Fig. 8(b)] with APTES. Figure 9 shows the necessary amount of Ni-Fers for single-grain formation ($D_{\text{Ni-Fers}}/D_{\text{grains}}$) on APTES. From the results, approximately 3.0×10^3 of Ni-Fers is necessary for single-grain formation on APTES at 0.50 mg/ml. For lower concentrations, results suggest that more Ni-Fers are necessary.

3.3 Positional control of crystallized areas

Finally, we tried the positional control of crystal grains. According to previous results, crystal grain shapes and sizes were markedly different with or without APTES at 0.05 mg/ml. Thus, Ni-Fers were prepared at 0.05 mg/ml, and ferritins adsorbed on 100, 50, and 10 μm square patterns of APTES. These samples were annealed at 550 °C for 24 h

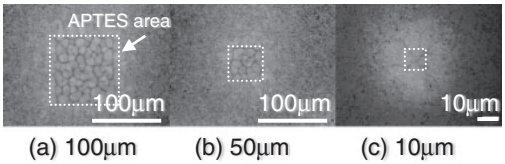

Fig. 10. Position-controlled poly-Si with (a) 100, (b) 50, and (c) 10 μm size APTES patterns.

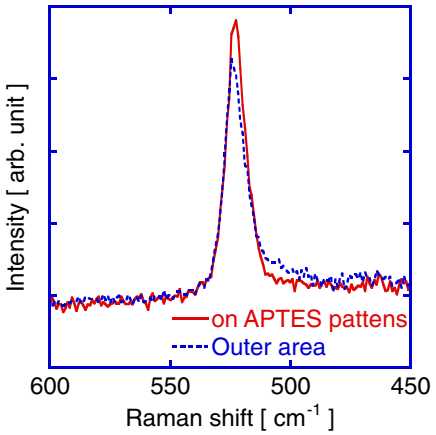

Fig. 11. (Color online) Raman spectra for APTES pattern and outer area.

after protein shell elimination, and grain boundaries were etching, by secco etchant as shown in Fig. 10. As a result, selective crystallizations were observed in the APTES-patterned areas. Crystallinities were investigated in APTES and surrounding areas by Raman spectroscopy, as shown in Fig. 11. As shown in Raman spectra, the peak at 520 cm^{-1} originating from crystalline silicon was confirmed, indicating that the whole surface was crystallized completely. However, areas outside the APTES patterns showed a weak signal at approximately 510 cm^{-1}. This signal is assigned to nano crystalline silicon. This means that areas outside the APTES patterns were crystallized from random nuclei by solid phase crystallization. On the other hand, crystal grains of approximately 12 μm were confirmed, and crystallization areas became smaller corresponding to the APTES pattern size. These results indicated that the location control of grain boundaries is possible by optimizing the APTES pattern and the condition of Ni-Fer solution.

4. Conclusions

We proposed a novel MILC process utilizing Ni oxide accommodated ferritins and their electrostatic interaction with APTES patterns. We investigated the adsorption densities of Ni-fers, crystal grain size, and densities with and without APTES. As a result, the adsorption densities and position of adsorption can be controlled by controlling Ni-Fer concentration. We confirmed that the location-controlled crystal grain formation corresponding to the APTES patterns. We succeeded in obtaining position-controlled poly-Si thin films.

Acknowledgements

This study is supported by the Core Research for Evolutional Science and Technology, Japan Science and Technology Agency.

1) W. S. Sohn, J. H. Choi, K. H. Kim, J. H. Oh, S. S. Kim, and J. Jang: J. Appl. Phys. **94** (2003) 4326.
2) I. Yamashita, J. Hayashi, and M. Hara: Chem. Lett. **33** (2004) 1158.
3) R. Tsukamoto, K. Iwahori, M. Muraoka, and I. Yamashita: Bull. Chem. Soc. Jpn. **78** (2005) 2075.
4) K. Iwahori, K. Yoshizawa, M. Muraoka, and I. Yamashita: Inorg. Chem. **44** (2005) 6393.
5) T. Dougras and M. Young: Nature **393** (1998) 152.
6) H. Kirimura, Y. Uraoka, T. Fuyuki, M. Okuda, and I. Yamashita: Appl. Phys. Lett. **86** (2005) 262106.
7) Y. Kuo and P. M. Kozlowski: Appl. Phys. Lett. **69** (1996) 1092.
8) Y. Tojo, A. Miura, T. Fuyuki, I. Yamashita, and Y. Uraoka: IMID 2009 Dig., 2009, p. 553.
9) K. Yoshizawa, K. Iwahori, K. Sugimoto, and I. Yamashita: Chem. Lett. **35** (2006) 1192.
10) S. Kumagai, S. Yoshii, K. Yamada, N. Matsukawe, I. Fujiwara, K. Iwahori, and I. Yamashita: Appl. Phys. Lett. **88** (2006) 153103.
11) K. Yamada, S. Yoshii, S. Kumagai, I. Fujiwara, K. Nishio, M. Okuda, N. Matsukawa, and I. Yamashita: Jpn. J. Appl. Phys. **45** (2006) 4259.